Data Extraction from Terahertz Time Domain Spectroscopy Measurements

Maik Scheller

Abstract The potential of terahertz (THz) time domain spectroscopy to simultaneously determine the complex dielectric parameters of materials and their geometrical thickness is of high interest for scientific spectroscopy and for general metrology. This paper provides an overview of the background of the data extraction from THz measurements and discusses the accuracy and ambiguity of this extraction process. It is shown that the signal to noise ratio of the measurement as well as the bandwidth of the accessible THz spectrum define the limitation of the achievable accuracy in the data extraction.

Keywords Terahertz · Thickness determination · Data analysis · Parameter extraction · Fabry-Perót

1 Introduction

Terahertz (THz) time domain spectroscopy (TDS) is a powerful technique for the characterization of samples in the THz frequency range. Employing ultra-short femtosecond laser systems allows for the generation and coherent detection of electromagnetic pulses with sub-ps duration which cover a frequency range beginning from sub-100 GHz to several THz [1]. Unlike incoherent measurement schemes, the TDS technique gives access to the complex electrical field of the THz waveform [2]. Thus, by comparing the waveform obtained from a propagation through free air (reference measurement) to the waveform which interacts with a device under investigation (sample measurement), it is possible to determine the complex dielectric material parameters of the sample over a broad frequency interval with a single measurement. However, to carefully make use of the full information buried in the raw measured data, a sophistic data analysis is required. The main obstacles are the interfering Fabry-Perót (FP)-echoes resulting from multiple internal reflections from the material-air interfaces. However, it has been shown that considering the (FP)-echoes in the data extraction allows for a simultaneous determination of the samples thickness and the material parameters [3].

M. Scheller (✉)
College of Optical Sciences, University of Arizona, 1630 East University Boulevard, Tucson, Arizona 85721, USA
e-mail: mscheller@optics.arizona.edu

This paper gives an overview of the data extraction process for THz TDS measurements. Moreover, the accuracy of the extracted data is discussed by studying the effects of the signal-to-noise ratio of the measurement as well as the bandwidth of the accessible THz spectrum. The discussion is focused on TDS transmission measurements as these provide in the case of transparent sample a higher sensitivity than reflection measurements [4]. However, the general scheme to analyze reflection measurements is similar and is discussed in more detail in [4,5].

2 Background

Figure 1 illustrates the general approach to characterize a sample with THz TDS in transmission geometry. First, a reference measurement is obtained which provides all of the information of the employed system characteristics. Then, the sample, placed within the beam path, is measured. The figure also shows the general shape of the two time domain signals of the reference and sample measurement. While the reference scan consists ideally only of a single pulse, the sample waveform exhibits multiple pulses, the directly transmitted pulse and the multiple FP echoes.

The following equations describe the time delays Δt_m between the reference pulse and the FP-echo pulses of order m for the case of an ideal non-dispersive sample with refractive index n and a thickness L [6]:

$$\begin{aligned}
m = 0: &\quad \Delta t_0 \propto (n-1)\,L\,, \\
m = 1: &\quad \Delta t_1 \propto (3n-1)\,L\,, \\
m = j: &\quad \Delta t_j \propto ((2j+1)n-1)L.
\end{aligned} \tag{1}$$

For simplicity, the refractive index of air in these and the following equations is approximated to be 1. Of most interest is that the time delay Δt_0 between the reference pulse and the pulse directly propagating through the sample and delay Δt_1 between the first FP-echo pulse
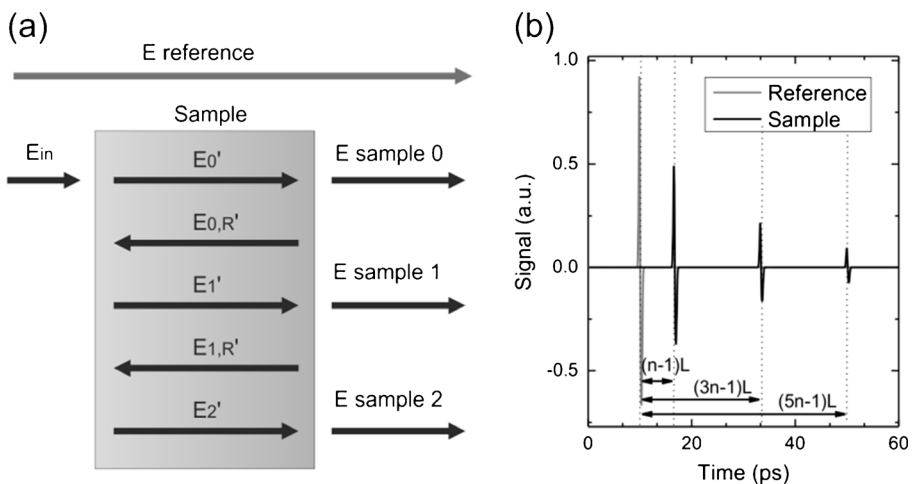

Fig. 1 (a) Illustration of the TDS measurements scheme. First, a reference pulse propagation through air (E reference) is measured. Afterwards, the sample is placed in the spectrometer and the signal is recorded which consists of the directly transmitted pulse (E sample 0) and the higher order FP reflections (E sample 1,2,...). (b) Idealized TDS signal: The pulse propagation through the sample pulse is delayed and attenuated compared to the reference pulse. Also, multiple FP echoes can be detected

and the reference are linear independent. Consequently, a single combination of n and L exists which satisfies this condition and thus, it is theoretically possible to extract the dielectric parameters of the sample and its thickness simultaneously from the measurement as long as at least one FP-echo pulse is present in the measured time window.

However, while a time domain analysis is primarily of use for fast process control of weakly-dispersive samples [6–8], a more detailed investigation requires more sophisticated approaches to extract the material parameters. This can most efficiently be done in the spectral domain. Here, the spectral transfer function $H(f)$ can be used to describes the interaction between a THz wave and the sample under investigation. This transfer function is defined as the ratio of the Fourier transforms of the sample measurement and the reference measurements. The advantage of this choice is that an analytical expression can easily be derived which only depends on the material parameters and not on the shape of the actual THz waveform which was used for the measurements. Analyzing the transfer function in spectral domain allows for an extraction of the frequency depended complex refractive index of the sample:

$$\widetilde{n}(f) = n(f) - i\kappa(f). \tag{2}$$

While the real part $n(f)$ describes the phase retardation induced by the sample, the imaginary part $\kappa(f)$ is a measure for the attenuation of the THz wave and can be used to deduct the absorption coefficient:

$$\alpha(f) = \frac{4\pi f}{c_0} \kappa(f), \tag{3}$$

where c_0 is the speed of light in vacuum. These optical parameter can easily be converted into the complex dielectric function:

$$\widetilde{\varepsilon}(f) = \widetilde{n}(f)^2. \tag{4}$$

Using the complex refractive index of the sample in combination with its thickness L allows for formulating the transfer function of the sample which takes the following form if the FP-echo pulses are neglected [9]:

$$\widetilde{R}_{AS}(f) = \left(\frac{n + i\kappa - 1}{n + i\kappa + 1} \right), \quad \widetilde{R}(f)_{SA} = -\left(\frac{n + i\kappa - 1}{n + i\kappa + 1} \right), \tag{5}$$

$$\widetilde{T}(f)_{AS} = \left(\frac{2}{n + i\kappa + 1} \right), \quad \widetilde{T}(f)_{SA} = \left(\frac{2n + 2i\kappa}{n + i\kappa + 1} \right), \tag{6}$$

$$\widetilde{P}(f) = \exp\left(-i\frac{2\pi f L(n + i\kappa - 1)}{c_0} \right), \tag{7}$$

$$\widetilde{H}(f) = \widetilde{T}(f)_{AS} \cdot \widetilde{P}(f) \cdot \widetilde{T}(f)_{SA}. \tag{8}$$

This form makes use of three complex coefficients describing the reflection $\widetilde{R}(f)$ and transmission $\widetilde{T}(f)$ properties of the air-sample (AS) and sample-air (SA) interfaces as well as the propagation $\widetilde{P}(f)$ through the sample.

But even this simplified transfer function which only describes the initial pulse transmitted through the sample does not allow for a direct analytically extraction of n and κ. However, if the sample thickness is large compared to the wavelength, a good approximation is to neglect the phase delay of the complex reflection and transmission coefficients. In this case, the optical sample parameters can directly be calculated if the geometrical sample thickness is known with the following equations:

$$n(f) = 1 + \frac{\angle \widetilde{H}(f)}{2\pi f L} c_0, \tag{9}$$

$$\kappa(f) = \frac{c_0}{2\pi f L} \ln \left(\frac{\left| \widetilde{H}(f) \right| (n+1)^2}{4 n_0} \right). \tag{10}$$

Yet, using these equations to analyze a measured transfer function disturbed by FP-echoes will yield a periodic oscillating artifact on the extracted parameters due to the interference fringes caused by the echoes as illustrated in Fig. 2.

To solve this problem in a simple matter, a time window may be used to filter out occurring FP-echoes. However, this reduces the frequency resolution and thus, spectral features such as absorption lines or dispersion effects are filtered out as well. To preserve the spectral information contained in the data the full time window of the measurement must be used. For this, the FP-echoes have to be included in the transfer function:

$$\widetilde{H}(f) = \widetilde{T}(f)_{AS} \widetilde{T}(f)_{SA} \sum_{g=0}^{M} \left(\exp \left(-i \frac{2\pi f L ((2g+1)[n+i\kappa]-1)}{c_0} \right) \cdot \widetilde{R}(f)_{SA}^{2g} \right). \tag{11}$$

Here, the number M denotes for the maximum FP-echo pulse order present within the time window of the measurement. The drawback of this more comprehensive description is that no direct analytical solution for the material parameter is possible and the equation has to be evaluated numerically.
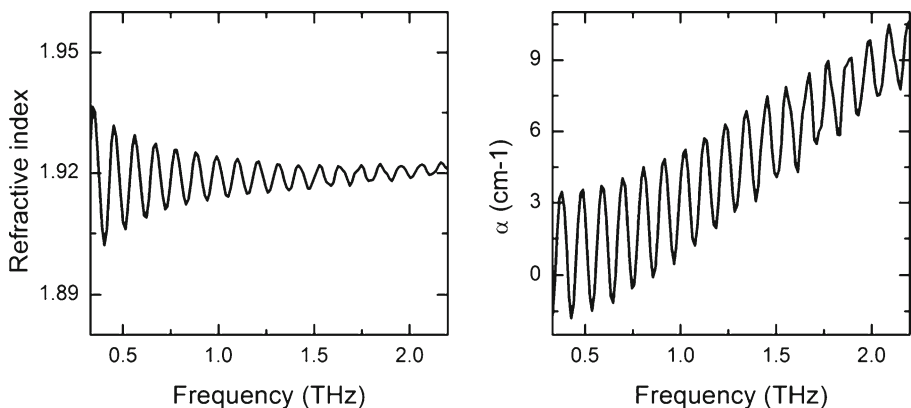

Fig. 2 Extracted refractive index of a 700 μm thick piece of fused silica using Eq. (9) and (10). The parameters are compromised by FP oscillations due to multiple echo pulses

To extract the material parameters, the following scheme has been proposed [3,9]: First an initial, fixed value for the thickness is assumed and initial values for the refractive index and the extinction coefficient are deducted in the frequency range of interest. Afterwards, for every frequency step the transfer function is calculated individually and compared to the measured transfer function. A numerical optimization procedure is used to optimize the values for n and κ to minimize the deviations between the calculated and the measured transfer function. This leads to the complex refractive index of the sample at a single frequency step. To extract the broadband dielectric function, the optimization has to be performed successively for every frequency step.

The problem here is that for every assumed initial thickness a numerically obtainable optimum for the complex refractive index exists. If the assumed thickness value deviates from the real thickness of the sample, the extracted refractive index and absorption coefficient are compromised by FP oscillations [9]. Only for the physical correct thickness the FP oscillations vanish.

Thus, the real physical thickness can be extracted by determining the material parameters for a set of possible thicknesses and minimizing the FP-oscillations. The simplest way to quantify the oscillation of the optical parameters is the total variation (TV) value [9] that is a measure of the variation in the optical parameters between neighboring sampling points:

$$TV = \sum_i \left| n(f_{i+1}) - n(f_i) \right| + \sum_i \left| \kappa(f_{i+1}) - \kappa(f_i) \right|. \tag{12}$$

If the extracted material parameters exhibit oscillations due to an incorrect thickness, the TV values will be higher than for the case of constant parameters. Yet, the period of the oscillations is inverse proportional to the samples thickness and is given by:

$$f_{FP} = \frac{c_0}{2Ln}. \tag{13}$$

In the case of samples only few hundreds of micrometer thick, the oscillation period is in the order of several hundred GHz to some THz and the variation induced by dispersion or absorption features can significantly exceed the amplitude of the FP-oscillations. Thus, the TV approach is not satisfying for the analysis of thin samples. More efficient is to selectively focus on the FP-oscillations by investigating the Fourier transform of the determined material parameters [10]. In this so called quasi-space (QS) the FP oscillations can easily be distinguished from other effects since the oscillations result in sharp and defined peaks. This approach, further depicted in [10], is illustrated in Fig. 3 for the case of a 54 μm thick piece of silicon. As can be seen in the figure, the FP oscillations on the material parameters result in a distinctive peak of the QS value which allows for identifying the optimal thickness of the sample. The QS scheme can also be applied to analyze thick samples effectively as the focus on the period of the FP-oscillations can be seen as a lock-in detection-scheme. This allows in general for an effective reconstruction of oscillations even in the presence of a relatively noise background.

Other methods for parameter extraction algorithms have been proposed e.g. to employ the Kramers-Kronig relation (KKR) for overcoming ambiguities in the data extraction [11]. However, the KKR requires information over the entire frequency range. Thus, for a realistic application to THz measurements with limited bandwidth, the KKR is only a good approximation for frequencies close to isolated absorption features and loses validity at the edges of the measured frequency window.

Besides pure frequency domain approaches, it is also possible to employ a hybrid technique [12] where the material parameters in frequency domain are used to compute the spectral transfer function. The sample response is then computed in frequency domain by
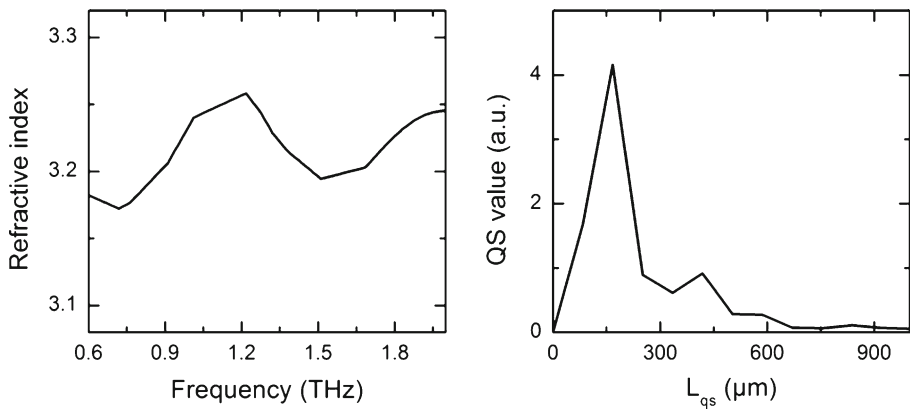
Fig. 3 (left) The extracted refractive index of an 54 μm thick piece of silicon for an incorrectly assumed thickness. (right) The corresponding QS value shows a pronounced peak due to the FP oscillations which can be employed to identify the real thickness of the sample

multiplication of the complex reference measurement with the transfer function. To reconstruct the time domain signal, an inverse Fourier transform is used. The reconstructed signal is compared to the sample measurement in time domain and the difference between the wave-forms gives an optimization values to extract the material parameters [12]. Yet, this method requires a large amount of computational Fourier transform operations.

A faster way to extract the data has been discussed in [13]. Here, the complex refractive index of the samples is determined by the approximation (9),(10) for an arbitrary thickness over the full frequency domain and then a filtered to remove the FP oscillations. The frequency dependent real and imaginary parts of the refractive index yield into two base vectors. These vectors as well as the thickness of the samples are then scaled by linear coefficients so that the parameter extraction over the full frequency range simplifies into a single 3D-optimization. Therefore, this approach may be adopted for real-time analysis, e.g. in THz imaging or process control. Yet, the filtering may affect the accuracy in presence of sharp absorption features.

The following section provides an example of a practical implementation of an extraction algorithm. Here, the focus lays on the QS evaluation due to its stability even though it requires a relatively high amount of computational iterations. However, it has been shown that this algorithm has the potential to rigorously determine the optimal parameters even if the samples are thinner than 100 micrometer [10].

3 Extraction Algorithm

As stated previously, initial values for the three unknown parameter n, κ and L have to be chosen. For the thickness, a rough estimate can typically made from a mechanical measure of the samples geometry. After an initial thickness L_0 is selected, the equations (9) and (10) can be used to determine initial values for the complex refractive index for every frequency step:

$$n_0(f) = 1 + \frac{\angle \widetilde{H}(f)}{2\pi f L_0} c_0, 0 \quad \kappa_0(f) = \frac{c_0}{2\pi f L_0} \ln\left(\frac{|\widetilde{H}(f)|(n_0+1)^2}{4n_0}\right). \quad (14)$$

However, in presents of FP oscillations, these derived parameters will be compromised by FP-oscillations. An efficient way to filter these out is to apply a band-stop filter on the values derived by (14), centered on the oscillations frequency f_{FP} as discussed in [13]. To obtain these frequency, it is either possible to spectrally average over the refractive index derived by (14) and calculate f_{FP} according to (13) or the make use of the oscillations of the transfer function induced by the FP-oscillations. Here, the QS scheme can be employed by applying a Fourier transform to $H(f)$:

$$QS_H(x_{QS}) := FFT\left(\left|\tilde{H}(f)\right|\right). \tag{15}$$

The argument x_{QS} is related to the optical thickness $L_{opt}=nL$ by:

$$L_{opt} = x_{QS}\frac{c_0}{2}. \tag{16}$$

The resulting QS value of $H(f)$ exhibits a pronounced maximum corresponding to the FP oscillations as illustrated in Fig. 4. Therefore, detecting the position x_{QS} of the maximum of QS_H allows for a direct determination of the oscillations period. The Fig. 4 shows also initial values for the complex refractive index before and after stop-band filtering. An estimate of the optical thickness of the sample is also required to determine the highest order M of FP-echoes which will be included in the time window of the measurement by using the Eq. (1).

The next step is to perform a 2-dimensional optimization of n and κ to minimize the derivation ΔH between the measured and the calculated transfer function for every frequency step, e.g. by the Nelder–Mead simplex method [14]:

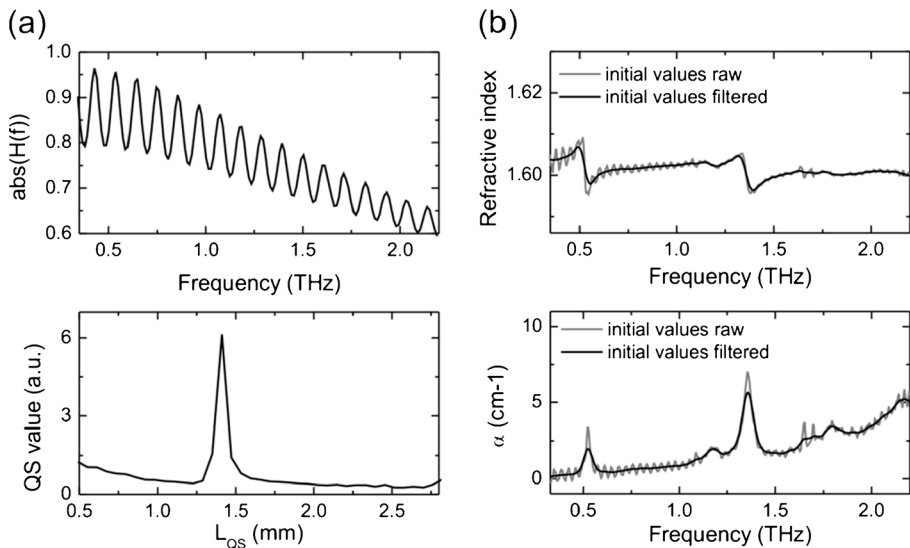$$\Delta H(f) = \sum_f \left|\tilde{H}_{theoretical}(f, n, \kappa) - \tilde{H}_{measured}(f)\right|. \tag{17}$$

Fig. 4 (a) Absolute value of the transfer function and corresponding QS value for a sample with 1.4 mm optical thickness. (b)Raw and filtered initial values of an alpha-lactose polymer mixture

This calculations needs to be performed for a series of thicknesses in the vicinity of L_0 to identify the real solution by the use of the QS method. Here, either the real or imaginary part of the refractive index can be used to derive the QS parameters n_{QS} and κ_{QS}.

$$QS_n(x_{QS}) := FFT(|n(f)|), \tag{18}$$

$$QS_\kappa(x_{QS}) := FFT(|\kappa(f)|). \tag{19}$$

The Fig. 5 shows the QS value (for x_{QS} corresponds to the optical sample thickness) as well as the extracted refractive index and extension coefficient for a sample for different thickness values. As can be seen in the figure, incorrect thicknesses yield into pronounced FP oscillations and high QS values. The QS value has a distinct minimum which allows for a rigorously conversion of this algorithm.

However, there are two limitations on the applicability of this procedure to simultaneous determine the thickness and the optical parameters. The first one is the finite frequency bandwidth and frequency resolution of the THz measurements. The FP-period in frequency space is inverse proportional to the samples thickness. For an extraction of the samples parameters as discussed before, the FP-period has to be observable in the measured spectrum. That means that the optical thickness of the sample has to be in the interval defined by the frequency bandwidth Δf and resolution df of the measurement:

$$\frac{c_0}{2\Delta f} \leq L_{opt} \leq \frac{c_0}{4df}. \tag{20}$$

While the upper limit corresponds to the Nyquist–Shannon sampling theorem and the occurrence of at least one echo pulse in the time window of the measurement, the lower constrain accounts for the distinguishability of the QS peak from its neighboring values and consequently for the condition of at least one single period of the oscillation being within the frequency bandwidth covered by the measurement.

Therefore, the range of determinable sample thickness is limited by the signal-to-noise ratio (SNR) of the measurement which determines the spectrometer's bandwidth. However, the SNR also limits the accuracy of the thickness determination. This can be described by studying
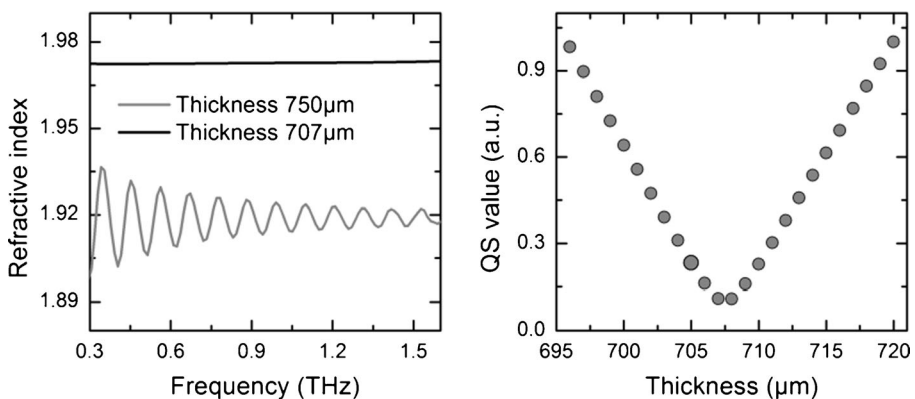

Fig. 5 (Left): Extracted refractive index of a 707 μm glass sample for two different assumed thicknesses. (Right): QS value for different thicknesses. A distinct minimum around 707 μm results which corresponds to a vanishing FP oscillation on the material parameters

the changes of the theoretical transfer function by slightly varying thickness δL around the ideal thickness L:

$$n_{\delta L} \approx 1 + (n-1)\frac{L}{L+\delta L}, \tag{21}$$

$$\kappa_{\delta L} \approx \kappa \frac{L}{L+\delta L}, \tag{22}$$

$$\widetilde{H}_{\delta L}(f) = \widetilde{T}_{\delta L}(f)_{AS}\widetilde{T}_{\delta L}(f)_{SA}\sum_{g=0}^{M}\left(\exp\left(-i\frac{2\pi f(L+\delta L)((2g+1)[n_{\delta L}+i\kappa_{\delta L}]-1)}{c_0}\right)\cdot\widetilde{R}_{\delta L}(f)_{SA}^{2g}\right), \tag{23}$$

where the deviating real and imaginary part of the refractive index $n_{\delta L}$ and $\kappa_{\delta L}$ are estimated based on Eq. (9) and (10). These values are also used to derivate the modified reflection and transmission coefficients $\widetilde{T}_{\delta L}$ and $\widetilde{R}_{\delta L}$. The maximal accuracy of the thickness determination is reached when the change of a thickness by δL yields into a change of $\widetilde{H}$ which is smaller than the standard variation of the measured transfer function:

$$\left|\widetilde{H}_L - \widetilde{H}_{\delta L}\right| \leq \left|\Delta\widetilde{H}_{measured}\right|. \tag{24}$$

Moreover, the accuracy of the extracted material parameters is limited by the noise in the system. A detailed analysis of the uncertainty in THz measurements, the dynamic range, and the dependence on the samples thickness can be found in [15–17]. One way to quantify the accuracy is to derive a confidence interval of the transfer function with an error propagation model as discussed in [18]. For this, the transfer function is expressed in a general complex form depending on the real values a,b,c,d:

$$\widetilde{H} := \frac{a+i\cdot b}{c+i\cdot d}. \tag{25}$$

This expression can be separated in its real and imaginary part:

$$re(a,b,c,d) := \mathrm{Re}\left\{\widetilde{H}\right\} = \frac{ac+bd}{c^2+d^2}, \tag{26}$$

$$im(a,b,c,d) := \mathrm{Im}\left\{\widetilde{H}\right\} = \frac{bc-ad}{c^2+d^2}. \tag{27}$$

The confidence interval $\Delta\mathrm{Re}\left\{\widetilde{H}\right\}$ and $\Delta\mathrm{Im}\left\{\widetilde{H}\right\}$ results from Gaussian error propagation of the standard derivations of the values a,b,c,d:

$$\Delta\mathrm{Re}\left\{\widetilde{H}\right\} = \sqrt{\left(\Delta a\frac{\delta re}{\delta a}\right)^2 + \left(\Delta b\frac{\delta re}{\delta b}\right)^2 + \left(\Delta c\frac{\delta re}{\delta c}\right)^2 + \left(\Delta d\frac{\delta re}{\delta d}\right)^2}, \tag{28}$$

$$\Delta\mathrm{Im}\left\{\widetilde{H}\right\} = \sqrt{\left(\Delta a\frac{\delta im}{\delta a}\right)^2 + \left(\Delta b\frac{\delta im}{\delta b}\right)^2 + \left(\Delta c\frac{\delta im}{\delta c}\right)^2 + \left(\Delta d\frac{\delta im}{\delta d}\right)^2}. \tag{29}$$
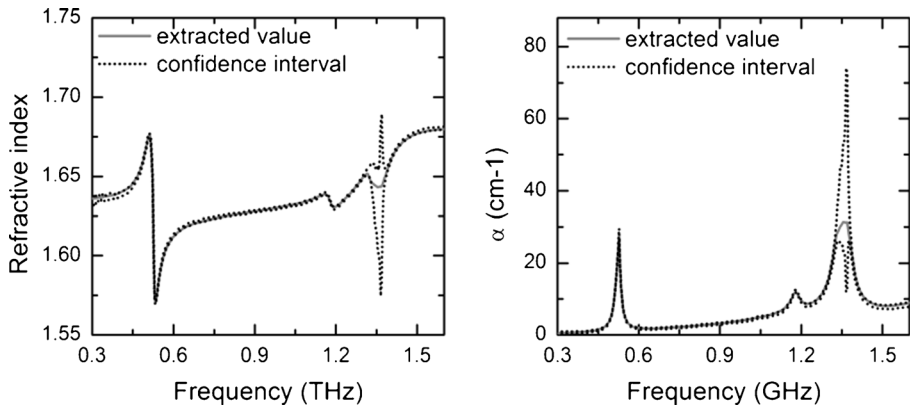
Fig. 6 Extracted refractive index and absorption coefficient of an alpha-lactose–polymer mixture which shows three absorption peaks in the observed frequency interval. Due to the reduced SNR at higher frequencies and the strong absorption, the confidence interval at 1.35 THz is rather large and must be considered in the interpretation of the extracted material parameters

To obtain the standard derivations of a,b,c,d it is necessary to perform multiple measurements of the sample and the reference scan as discussed in [18].

This confidence interval transfers to the extracted optical material parameters. Their accuracy is limited by the interval where the noise induces at least the same amount of variance to the measured transfer function as a change in the material parameter to the theoretical transfer function does:

$$\left| \widetilde{H}\left(f, n_{optimal}, \kappa_{optimal}\right) - \widetilde{H}\left(f, n_{optimal} \pm \Delta n, \kappa_{optimal} \pm \Delta\kappa\right) \right| \leq \left| \Delta\widetilde{H}_{measured}(f) \right|. \quad (30)$$

Therefore, for interpreting the extracted data it is necessary to consider the confidence interval as the extraction can easily yield in artifacts due to the limited dynamic range of the system as illustrated in Fig. 6.

4 Conclusion

The article discusses the fundamentals of the extraction of material parameters of THz time domain spectroscopy measurements. A brief guideline through the general scheme of an extraction algorithm is provided including the derivation of initial values and the basics of the optimization methods. It is shown that the thickness has to be determined carefully to avoid oscillating artifacts on the extracted material parameters. Moreover, the accuracy of the derived parameters and the limitation of the thickness determination are discussed.

References

1. P. Jepsen, D. G. Cooke, and M. Koch," Terahertz spectroscopy and imaging – Modern techniques and applications", Laser & Photonics Review 5, 124 (2011)
2. D. H. Auston and K. P. Cheung, "Coherent time-domain far-infrared spectroscopy," J. Opt. Soc. Am. B 2, 606-612 (1985).
3. L. Duvillaret, F. Garet and J. Coutaz, "Highly Precise Determination of Optical Constants and Sample Thickness in Terahertz Time-Domain Spectroscopy", Appl. Opt., 38, 409–415 (1999).

4. M. Bernier, F. Garet, J. Coutaz, "Precise Determination of the Refractive Index of Samples Showing Low Transmission Bands by THz Time-Domain Spectroscopy," IEEE Transactions on Terahertz Science and Technology, 3, 295–301 (2013).

5. E. Vartiainen, Y. Ino, R. Shimano, M. Kuwata-Gonokami, Y.P. Svirko, K-E. Peiponen, "Numerical phase correction method for terahertz time-domain reflection spectroscopy," Journal of Applied Physics, 96, 4171–4175 (2004).

6. M. Scheller, and M. Koch, "Fast and accurate thickness determination of unknown materials using terahertz time domain spectroscopy," J. of Infrared, Millimeter, and Terahertz Waves 30, 762-769 (2009).

7. T. Yasui, T. Yasuda, K. Sawanaka and T. Araki, "Terahertz paintmeter for noncontact monitoring of thickness and drying progress in paint film", Appl. Opt., 44, 6849-6856 (2005)

8. T. Yasuda, T. Iwata, T. Araki, and T. Yasui, "Improvement of minimum paint film thickness for THz paint meters by multiple-regression analysis," Appl. Opt. 46, 7518–7526 (2007)

9. T. D. Dorney, R. G. Baraniuk and D. M. Mittleman, "Material parameter estimation with terahertz time-domain spectroscopy", J. Opt. Soc. Am. A 18, 1562–1571 (2001).

10. M. Scheller, C. Jansen and M. Koch, "Analyzing Sub-100 μm Samples with Transmission Terahertz Time Domain Spectroscopy", Opt. Commun. 282, 1304–1306 (2009).

11. M. Krüger, S. Funkner, E. Bründermann, and M. Havenith. Uncertainty and ambiguity in terahertz parameter extraction and data analysis. Journal of Infrared, Millimeter, and Terahertz Waves 32, 699-715 (2011).

12. Xiangjun Lia, Zhi Hongb, Jinlong Heb, Yuquan Chena, "Precisely optical material parameter determination by time domain waveform rebuilding with THz time-domain spectroscopy," Optics Communications 283, 4701–4706 (2010)

13. M. Scheller, "Real-time terahertz material characterization by numerical three-dimensional optimization," Opt. Express 19, 10647–10655 (2011)

14. J. C. Lagarias, J. A. Reeds, M. H. Wright, and P. E. Wright, "Convergence properties of the nelder–mead simplex method in low dimensions", SIAM J. on Optimization 9, 112–147 (1998).

15. P. U. Jepsen and B. M. Fischer, "Dynamic range in terahertz time-domain transmission and reflection spectroscopy," Opt. Lett. 30, 29–31 (2005).

16. W. Withayachumnankul, B. M. Fischer, H. Lin, and D. Abbott, "Uncertainty in terahertz time-domain spectroscopy measurement," J. Opt. Soc. Am. B 25, 1059–1072 (2008)

17. Withawat Withayachumnankul, Bernd M. Fischer, and Derek Abbott, "Material thickness optimization for transmission-mode terahertz time-domain spectroscopy," Opt. Express 16, 7382–7396 (2008)

18. I. Pupeza, R. Wilk, and M. Koch, "Highly accurate optical material parameter determination with THz time-domain spectroscopy," Opt. Express 15, 4335-4350 (2007)